Since January 2020 Elsevier has created a COVID-19 resource centre with free information in English and Mandarin on the novel coronavirus COVID-19. The COVID-19 resource centre is hosted on Elsevier Connect, the company's public news and information website.

Chemical Engineering Journal 428 (2022) 131408

Contents lists available at ScienceDirect

Chemical Engineering Journal

journal homepage: www.elsevier.com/locate/cej

Oxidation of chloroquine drug by ferrate: Kinetics, reaction mechanism and antibacterial activity

Feilong Dong [a], Jinzhe Li [a], Qiufeng Lin [b], Da Wang [a], Cong Li [c], Yi Shen [a], Tao Zeng [a], Shuang Song [a,*]

[a] Key Laboratory of Microbial Technology for Industrial Pollution Control of Zhejiang Province, College of Environment, Zhejiang University of Technology, Hangzhou, 310014, China
[b] Department of Earth and Environmental Studies, Montclair State University, Montclair, NJ 07043, United States
[c] School of Environment and Architecture, University of Shanghai for Science and Technology, Shanghai, 200433, China

ARTICLE INFO

Keywords:
Chloroquine
Ferrate
Kinetics
Reaction pathways
Biodegradability

ABSTRACT

Chloroquine (CLQ) is required to manufacture on a larger scale to combat COVID-19. The wastewater containing CLQ will be discharged into the natural water, which was resistant to environmental degradation. Herein, the degradation of CLQ by ferrate (Fe(VI)) was investigated, and the biodegradability of the oxidation products was examined to evaluate the potential application in natural water treatment. The reaction between CLQ and Fe(VI) was pH-dependent and followed second-order kinetics. The species-specific rate constant of protonated Fe(VI) species ($HFeO_4^-$) was higher than that of the FeO_4^{2-} species. Moreover, increasing the reaction temperature could increase the degradation rate of CLQ. Besides, HCO_3^- had positive effect on CLQ removal, while HA had negative effect on CLQ removal. But the experiments shows Fe(VI) could be used as an efficient technique to degrade co-existing CLQ in natural waters. During the oxidation, Fe(VI) attack could lead to aromatic ring dealkylation and chloride ion substitution to form seven intermediate products by liquid chromatography-time-of-flight-mass spectrometry (LC-TOF-MS) determination. Finally, a pure culture test showed that the oxidation of CLQ by Fe(VI) could slightly increase the antimicrobial effect towards *Escherichia coli (E.coli)* and reduce the toxicity risk of intermediates. These findings might provide helpful information for the environmental elimination of CLQ.

1. Introduction

Malaria disease is the most widespread and essential parasitic disease in human [1–3]. Chloroquine (CLQ), as the primary antimalarial prevention drug, is widely administrated to treat all types of malarial infections [4]. Currently, CLQ has attracted increasing attention for COVID-19 treatment due to its low price and significant improvement of immune system [5–7]. It is required to manufacture this drug on a larger scale to combat COVID-19 that infected millions of people. Hence, a large amount of medical wastewater polluted by CLQ will be discharged into the environment. CLQ has been detected in aquatic environment at concentrations ranging from ng/L to μg/L. Olaitan et al. (2014) found that the median concentration of CLQ identified in different water samples from Nigeria was 2.12 μg/L [8]. However, like many antibiotics such as ciprofloxacin, erythromycin, penicillin and sulphisoxazole, CLQ has high potential to be persistent and bioaccumulative, hard to remove in waste [9]. Besides, due to the antiviral and antibacterial characteristics, CLQ can be transferred to biological organisms in a more toxic way and becomes a persistent emerging micropollutant in the futural surface water [10,11]. The high risk of the pollution necessitates more attention to limit its harmful effects on human health and the environment, including ozone-depleting substances [12,13], heavy metal bioaccumulation and persistence [14,15]. Therefore, there is an urgent demand for development of technically viable, low-cost, and energy-saving alternatives for CLQ elimination in water.

The previous studies only focused on the chemical stability and detection methods of CLQ in water [16–18], few researches concerned about the oxidation and fate of CLQ. Nord et al. found CLQ was photochemical degraded on irradiation with 240–600 nm light in aqueous solutions (pH 7.4), leading to N-dealkylation [19]. Kanakapura et al. investigated the forced degradation of CLQ in water by acid,

* Corresponding author.
E-mail address: ss@zjut.edu.cn (S. Song).

https://doi.org/10.1016/j.cej.2021.131408
Received 13 May 2021; Received in revised form 3 July 2021; Accepted 15 July 2021
Available online 8 August 2021

alkaline, peroxide, heat and light-induced. CLQ was degraded by 50% under alkaline hydrolysis conditions. Besides, Coelho et al. developed a degradation study submitting CLQ to alkaline hydrolysis and chemical oxidation with diluted H_2O_2 [9]. Recently, Sondos et al. used the electro-Fenton method to achieve high-efficiency degradation of CLQ in wastewater, which was as high as 92% under optimal conditions [11]. However, established drinking water treatment technologies cannot provide a sustainable solution to CLQ pollution. Thereby, it is necessary to find an efficient drinking water treatment technology to eliminate or reduce the harm of CLQ in surface water to respond to the huge usage of CLQ.

Ferrate (Fe(VI)) has been demonstrated for treating drinking water with the function of oxidation, flocculation, sterilization, disinfection and algae removal [20–22]. Fe(VI) is a strong oxidant with supercharged iron molecule, which has the redox potential of 2.20 V and 0.78 V in acidic and alkaline, respectively [23,24]. Compared with the common oxidants (e.g., permanganate, ozone, and hypochlorite), Fe(VI) has recently been shown to react with electron-rich organic moieties including pharmaceuticals [25–27]. In addition, Fe(VI) is similar to permanganate, the reduction product of ferric ion will transform into ferric hydroxide, which can be used as an in-situ coagulant in the subsequent coagulation [28–30]. Fe(VI) is environmentally friendly for treating water without producing secondary pollution [31]. In recent years, researches on the oxidation of antibiotics by Fe(VI) have been forthcoming, including the reaction kinetics, but the knowledge of antimalarial drugs (e.g., CLQ) and products of the oxidations under natural water conditions are very limited [32,33]. Significantly, due to the high toxicity and biological resistance of degradation products, the removal may not necessarily obviate the antibacterial properties completely [34,35]. After oxidation of the parent drug molecule, the antibacterial activity of reaction products is also missing in the literature.

The objectives of this study were to: (1) investigate the oxidation of CLQ by Fe(VI) at different Fe(VI) concentrations and temperature; (2) determine the reactions of Fe(VI) and CLQ by studying the kinetics of oxidation (species-specific rate constants) as a function of pH; (3) identify the high molecular weight transformation byproducts of CLQ by Fe(VI) treatment and propose the potential degradation pathways; and (4) evaluate the antibacterial activity of the reaction mixtures against *Escherichia coli* (*E.coli*).

2. Materials and methods

2.1. Standards and reagents

CLQ and diammonium 2,2′-azinobis-(3-ethylbenzothiazoline-6-sulfonate) (ABTS) were obtained from Aladdin Industrial Corporation (Shanghai, China) with purity higher than 98%. K_2FeO_4 of high purity (>92%) was synthesized by a wet oxidation method in the laboratory [36]. The Fe(VI) stock solutions were freshly prepared within 30 min prior to their use. Other reagents at least analytical purity including disodium hydrogen phosphate (Na_2HPO_4), sodium dihydrogen phosphate (NaH_2PO_4), sodium tetraborate decahydrate (Na_2BO_4), sodium chloride (NaCl), sodium nitrate ($NaNO_3$), sodium bicarbonate ($NaHCO_3$), sulphuric acid (H_2SO_4), glacial acetic acid (CH_3COOH) and sodium thiosulfate ($Na_2S_2O_3$) were purchased from Sigma-Aldrich (St. Louis, USA). Purified water was provided from JD Co. (Beijing, China). All the buffer solution was prepared using phosphate and borate to adjust the pH from 6.5 to 10.5.

2.2. Experimental procedures

The degradation experiments of CLQ were conducted in a 100 mL brown reagent bottle equipped with a magnetic stirring (500 r/min) at different temperatures (5, 10, 15, 20 and 25 °C). Reagents containing phosphate and borate were used to adjust the pH (7.3, 7.8, 8.2, 8.6, 9.0, 10.2) of the reaction solutions. The stock solutions of Fe(VI) (10 mM) were freshly prepared by dissolving solid K_2FeO_4 in pH 9.0 buffer (5 mM disodium hydrogen phosphate and 1 mM borate). The Fe(VI) stock solution was initially added to suspensions containing CLQ under rapid mixing. The initial concentration of Fe(VI) was controlled as 40, 90, 120, 150 and 180 μM while CLQ concentration was 10 μM. After reaction of 1.0, 3.0, 5.0, 7.0, 10.0, 15.0 and 20.0 min, 1 mL of the reaction solution was sampled and quenched with 0.1 mL sodium thiosulfate (3 mM) to detect residual CLQ concentrations. Meanwhile, 1 mL of the reaction solution was sampled to mix with 1 mL ABTS, 5 mL buffer solution (containing 0.6 M acetate and 0.2 M phosphate) and 19 mL purified water to detect the Fe(VI) concentrations by using the ABTS method at 415 nm [37]. Fig. S2 shows the adsorption capacity for CLQ by $Fe(OH)_3$ or Fe_2O_3, which formed by Fe(VI) decomposition. The result indicated $Fe(OH)_3$ or Fe_2O_3 formed by Fe(VI) decomposition had almost no adsorption capacity for CLQ.

The experiments of intermediate products identification were conducted in a 100 mL reaction suspensions of 10 μM CLQ and 150 μM Fe (VI) with pH 9.0 at room temperature (25 ± 1 °C). After 2 h, 60 mL samples were quenched with 1 mL sodium thiosulfate (10 mM) and stored at 4 °C for further analysis. All the experiments were carried out in triplicate. The average dates and the standard deviation were presented.

2.3. Analytical methods

The concentration of CLQ was determined by high-performance liquid chromatography (HPLC; Waters Corporation, USA) equipped with a Waters 2489 UV/Visible Detector and a XDB-C18 column (150 mm × 4.6 mm, 5 μm, Agilent Zorbax). The mobile phase for the measurement consisted of 0.1% (v/v) formic acid and acetonitrile at the ratio of 90:10 (v/v) with a flow rate of 1.0 mL/min. The detector temperature and wavelength were set at 40 °C and 340 nm, respectively. The limit of detection (LOD) for CLQ was 20 μg/L. The concentration of Fe(VI) was calculated using the ultraviolet–visible spectrophotometer (Beijing General Instruments Company Ltd, China) by sampling 1 mL solution to mix with 1 mL ABTS, 5 mL buffer solution (containing 0.6 M acetate and 0.2 M phosphate) and 19 mL deionized water to detect the Fe(VI) concentrations at 415 nm according to Eq. (1).

$$[Fe(VI)]_{sample} = \frac{\Delta A_l^{415} V_{final}}{\varepsilon l V_{sample}} \quad (1)$$

The concentrations of intermediate products were extracted by liquid/liquid extraction with n-hexane (ultra resi-analysed grade) and then evaporated on a rotatory evaporator (temperature at 45 °C, rotor speed of 80 rpm) to a volume less than 2 mL. Then, the sample was identified by liquid chromatography-time-of-flight-mass spectrometry (LC-QTOF-MS/MS) equipped with a Waters cortecs C18 column (2.1 × 50 mm, 1.7 μm). The mobile phase consisted of 0.1% formic acid and acetonitrile (90:10, v/v) with 0.3 mL/min flow rate. The MS system was operated at ESI^+ mode, capillary voltage 4 kV, gas temperature 150 °C, drying gas 15 L/min, sheath gas temperature 350 °C and sheath gas flow 12 L/min. The detection m/z range was from 100 to 500 and the scan time was 0.1 s.

2.4. Antibacterial activity assay

According to the previous study, the methods with *E. coil* were used for determining the biotoxicity of Fe(VI), CLQ and their oxidation products [38]. The experiment was carried out under the specific condition: 10 μM CLQ solution was reacted with Fe(VI) at the molar ratio of 18:1, the temperature was controlled as 25 °C. Four groups were set as follow: the control groups (adding 2 mL purified water into 20 mL of Luria-Bertani (LB) medium), the Fe(VI) decomposition groups (180 μM Fe(VI) dissolved in 100 mL purified water and decomposition for 12 h,

then, 2 mL sample filtered through the hydrophilic acetate fiber membrane (0.45 μm) was added into 20 mL of LB medium), the CLQ groups (2 mL of sterile CLQ solution (10 μM) was added into 20 mL of LB medium), the experiment groups (Fe(VI):CLQ = 18:1, Fe(VI) reacted with CLQ for 12 h, 2 mL sample filtered through the hydrophilic acetate fiber membrane (0.45 μm) was added into 20 mL of LB medium). Then, *E. coli* in exponential phase was inoculated into the reactors. The optical density value of bacterial growth was determined by the absorbance of 600 nm using a UV–Visible spectrophotometry (T6 New century).

3. Results and discussion

3.1. Influence of Fe(VI) concentration on CLQ degradation

The fate for CLQ degradation was reacted with K_2FeO_4 in the various forms. To examine the role of the initial concentration of K_2FeO_4 on CLQ degradation, different molar ratios of [Fe(VI)]/[CLQ] varied between 4 and 18 were carried in the buffered solution at pH 9.0. As shown in Fig. 1a, the degradation rate of CLQ increased with the increasing initial concentration of Fe(VI). When the molar ratios of [Fe(VI)]/[CLQ] were 4, 9, 12, 15 and 18, the degradation efficiencies of CLQ were 17.9%, 52.1%, 72.3%, 85.8% and 100% within 10 min, respectively. This phenomenon was attributed to the increased amount of Fe(VI) available to oxidize CLQ. Fig. 1b shows the final removal efficiencies of CLQ upon different molar ratios of [Fe(VI)]/[CLQ]. The final removal efficiencies of CLQ were 32.4% and 67.6% at the molar ratio of 4 and 9, respectively. At a molar ratio of 12:1 ([Fe(VI)]/[CLQ]), more than 90% of CLQ was eliminated. The results might be explained by considering simultaneous self-decomposition of Fe(VI) during the reaction (Fig. S3). The degradation of CLQ by Fe(VI) was slower than the simultaneous self-decomposition of Fe(VI), meaning that a high amount of Fe(VI) was needed to fully oxidize the CLQ. With the molar ratio greater than 12, the increase in removal became slower and almost complete removal of CLQ were observed at a molar ratio of 15 and 18. The half-lives at different molar ratios of [Fe(VI)]/[CLQ] were calculated using the solid line of Fig. 1b. In addition, Fig. S4 shows the extent of CLQ mineralization by Fe(VI) oxidation. The total organic matter (TOC) of the untreated water was 6.8 ± 0.1 mg/L. The TOC partial rapidly decreased after the Fe(VI) addition in the initial 1 h. Then, the TOC continued to slowly decrease with the prolonging of oxidation time. The higher the Fe (VI)/CLQ molar ratio, the more the TOC reduction. This result indicated only partial CLQ could be mineralized by Fe(VI) oxidation. Based on the data presented, the following pseudo-first-order rate (Eq. (2)) was proposed to verify further the effect of self-decomposition of Fe(VI) on the degradation of CLQ.

$$ln(\frac{[CLQ]_T}{[CLQ]_0}) = -k_{obs}t \quad (2)$$

Plots of $\ln([CLQ]_0/[CLQ]_t)$ with t was established in Fig. S5. When the molar ratio of [Fe(VI)]/[CLQ] was more than 9, the linear correlation was higher than 0.946, which fitted the pseudo-first-order well. However, the linear correlation was unsatisfactory ($R^2 = 0.882$) when the molar ratio of [Fe(VI)]/[CLQ] was 4. This result was consistent with the above explanation about the self-decomposition of Fe(VI) (Fig. S3).

3.2. Influence of pH on CLQ degradation

Preliminary evaluation of CLQ degradation over a wide pH range (4–11) were conducted using the following buffers: citrate for pH 3.5, acetate for 5.5, phosphate and borate for 6.5–10.5. The instability of Fe (VI) under acidic conditions (pH 4.0–7.0) led to the rapid degradation of CLQ (data not shown). Therefore, alkaline conditions (pH = 7.0–11.0) for CLQ degradation were further investigated. The experiments carried out within the pH of 7.3, 7.8, 8.2, 8.6, 9.0 and 10.2. The molar ratio of ([Fe(VI)]/[CLQ]) was controlled as 15:1.

Previous studies have demonstrated that the reaction rate for the Fe (VI) oxidation with organic compound follows second-order reaction kinetics [24,39]. Thereby, the reaction rate constant for the CLQ degradation by Fe(VI) can be expressed as

$$-\frac{d[CLQ]}{dt} = k_{app}[Fe(VI)][CLQ] \quad (3)$$

$$ln(\frac{[CLQ]}{[[TCS]_0]}) = -k_{app}\int_0^t [Fe(VI)]dt \quad (4)$$

where k_{app} is the overall apparent reaction rate constant, [Fe(VI)] and [CLQ] are the concentration of Fe(VI) and CLQ, respectively. Fig. 2a shows the values of k_{app} at different pH (7.3–10.2). Rates for the CLQ degradation by Fe(VI) decreased with an increase in pH, which was consistent with the reactions of antibiotics by Fe(VI) [33]. The rate constant was 7.7×10^2 $M^{-1}s^{-1}$ at pH 7.3 and decreased dramatically from pH 7.8 ($k_{app} = 1.9 \times 10^2$ $M^{-1}s^{-1}$) to 10.9 ($k_{app} = 18$ $M^{-1}s^{-1}$). The values of k_{app} were pH-dependent, which could be attributed to the species of both Fe(VI) and CLQ. According to the Eqs. (5) to (9), in the pH range of 7.3–10.2, Fe(VI) and CLQ both have two acid–base species, which were $HFeO_4^-$, FeO_4^{2-} and CLQ^-, CLQ^{2-}, respectively.

$$H_3FeO_4^+ \rightarrow H_2FeO_4 + H^+ \quad pK_1 = 1.5 \quad (5)$$

$$H_2FeO_4 \rightarrow HFeO_4^- + H^+ \quad pK_2 = 3.5 \quad (6)$$

$$HFeO_4^- \rightarrow FeO_4^{2-} + H^+ \quad pK_3 = 7.2 \quad (7)$$

$$CLQ \rightarrow CLQ^- + H^+ \quad pK_{a1} = 8.1 \quad (8)$$

$$CLQ^- \rightarrow CLQ^{2-} + H^+ \quad pK_{a2} = 10.2 \quad (9)$$

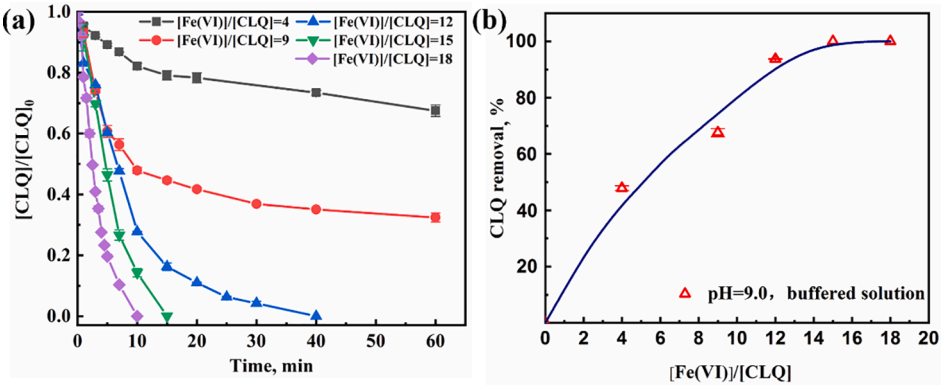

Fig. 1. The effect of [Fe(VI)]/[CLQ] on the degradation efficiency of CLQ (a) and the effect of [Fe(VI)]/[CLQ] on the final removal efficiency of CLQ (b). (The ratio of [Fe(VI)]/[CLQ] = 4, 9, 12, 15, 18, initial CLQ concentration = 10 μM, pH = 9, T = 25 °C).

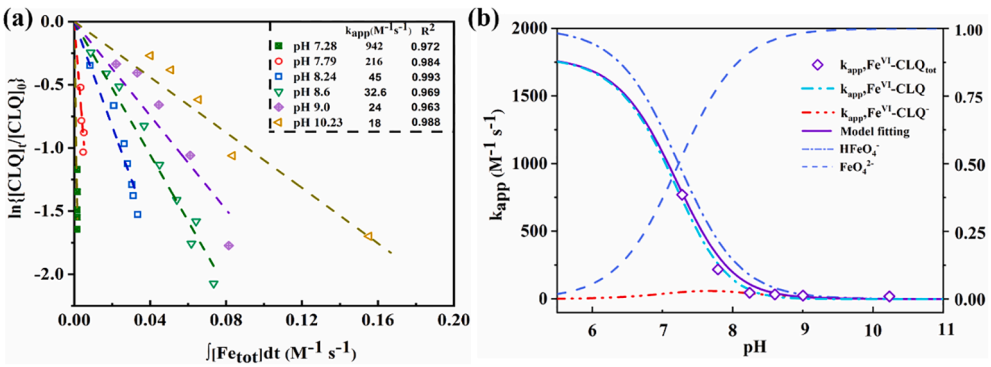

Fig. 2. The effect of pH on the degradation efficiency of CLQ (a) and the model fitting result of the second-order reaction rate constant of ferrate with CLQ (b). (The ratio of [Fe(VI)]/[CLQ] = 15:1, initial CLQ concentration = 10 μM, pH = 7.3, 7.8, 8.2, 8.6, 9.0 and 10.2, T = 25 °C).

The CLQ degradation by Fe(VI) contributed to four possible reactions as follow.

$$HFeO_4^- + CLQ \rightarrow Fe(III) + Products\ k_1 \quad (10)$$

$$HFeO_4^- + CLQ^- \rightarrow Fe(III) + Products\ k_2 \quad (11)$$

$$FeO_4^{2-} + CLQ \rightarrow Fe(III) + Products\ k_3 \quad (12)$$

$$FeO_4^{2-} + CLQ^- \rightarrow Fe(III) + Products\ k_4 \quad (13)$$

Thus, the pH dependence of k_{app} can be calculated by Eq.(14).

$$-\frac{d[Fe(VI)]_{tot}}{dt} = k[Fe(VI)]_{tot}CLQ_{tot} = k_1[HFeO_4^-][CLQ] + k_2[HFeO_4^-][CLQ^-] + k_3[FeO_4^{2-}][CLQ] + k_4[FeO_4^{2-}][CLQ^-] \quad (14)$$

where k_1, k_2, k_3, and k_4 represent species-specific rate constants for reactions ((2)–(5)), respectively. The calculation of k_{app} can be simplified as (Eqs (15) and (16)):

$$k_{app} = \sum_{i=1,2 j=1,2} k_{ij}\alpha_i\beta_j[Fe(VI)]_{tot}[(CLQ)]_{tot} \quad (15)$$

$$k_{app} = k_{11}\alpha_1[HFeO_4^-]\beta_1[CLQ] + k_{12}\alpha_1[HFeO_4^-]\beta_2[CLQ^-] + k_{21}\alpha_2[FeO_4^{2-}]\beta_1[CLQ] + k_{22}\alpha_2[FeO_4^{2-}]\beta_2[CLQ^-] \quad (16)$$

where the α_i, β_j are the respective species distribution coefficient for Fe (VI) and CLQ while i, j each represents the corresponding two species of Fe(VI) and CLQ. The value of α_i, β_j can be calculated as follow.

$$\alpha_1[HFeO_4^-] = [HFeO_4^-]/[Fe(VI)]_{tot} = [H^+]/([H^+] + 10^{-7.23}) \quad (17)$$

$$\alpha_2[FeO_4^{2-}] = [FeO_4^{2-}]/[Fe(VI)]_{tot} = [10^{-7.23}]/([H^+] + 10^{-7.23}) \quad (18)$$

$$\beta_1[CLQ] = [CLQ]/[CLQ]_{tot} = [H^+]/([H^+] + 10^{-8.1}) \quad (19)$$

$$\beta_1[CLQ^-] = [CLQ^-]/[CLQ]_{tot} = [10^{-8.1}]/([H^+] + 10^{-8.1}) \quad (20)$$

Based on the least-squares nonlinear regressions of the experimental k_{app} data, the second-order rate constants of k_1, k_2, k_3, and k_4 were calculated as 1792, 82, 0 and 0 $M^{-1}s^{-1}$, respectively. The Fitting of the experimental data in Fig. 2b could describe very well with the experimental k_{app} ($R^2 = 0.98$). The aforementioned date indicated that: (1), no significant reaction between the $HFeO_4^-$ and CLQ^- occurred and the reaction of $HFeO_4^-$ controlled the overall rate of reaction; (2) the contribution of unprotoned ferrate and CLQ was not obvious and could be neglected. Therefore, the pH dependence of k_{app} for CLQ could be considered as the reactions of $HFeO_4^{2-}$ with CLQ and CLQ^-. According to the different speciation of Fe(VI), the molar fraction of $HFeO_4^-$ decreases and that of FeO_4^{2-} increases with the increasing pH [40]. Meanwhile, the protonated form of Fe(VI) has a larger spin density on the oxo ligands than the unprotonated form of Fe(VI), which increases the oxidation ability of protonated Fe(VI) [41]. In addition, the steadline in Fig. 2b shows that Eqs. (10) and (11) were mainly contributed to the CLQ degradation. The protonated CLQ reaction with $HFeO_4^-$ was faster than the unprotonated CLQ^- ($k_2 > k_3$).

3.3. Influence of temperature on CLQ degradation

The self-decomposition of Fe(VI) was related to the reaction temperature [42]. The effect of temperature on the CLQ degradation by Fe (VI) was varied from 5 °C to 25 °C at pH 9.0. As shown in Fig. 3a. The rate of CLQ degradation increased with increasing temperature. According to the pseudo-first-order rates in Fig. S6, the k_{obs} of CLQ were increased from 0.034 $M^{-1}min^{-1}$ to 0.200 $M^{-1}min^{-1}$ while the temperature increased from 5 °C to 25 °C. There were two reasons contributed to this phenomenon. On the one hand, the increase of temperature would promote the Fe(VI) self-decomposing into the intermediate oxidants (Fe(VI)) and Fe(V)), which had more vital oxidation ability. In previous work, Wagner et al. found that Fe(VI) was much more stable at 0.5 °C than at 25 °C [42]. On the other hand, the increase in temperature increased the collision frequency between Fe(VI) and the target pollutant, which increased the elimination rate of CLQ [43]. Arrhenius equation was used to calculate the activation energy of CLQ degradation by Fe(VI) (Eq. (21)).

$$k_{Obs} = Aexp^{-\frac{E_a}{RT}} \quad (21)$$

$$ln(k_{Obs}) = ln(A) - \frac{E_a}{RT} \quad (22)$$

where R is the universal gas constant in 8.314 J/mol·K. Based on the experimental data, the rate constant for CLQ degradation can be estimated as follows:

$$ln(k_{Obs}) = -5137.4(\frac{1}{T}) + 21.972 \quad (23)$$

The ln k_{obs} and 1/T showed a satisfied correlation, which was higher than 0.97. The activation energy was calculated as 63.5 kJ/mol. Therefore, the higher temperature was prone to degradation the CLQ by Fe(VI).

3.4. CLQ degradation in natural water constituents

Various inorganic anions are ubiquitously existing in natural water, including Cl^-, NO_3^- and HCO_3^-, which can affect the environmental elimination of organic pollutants. In this study, the effects of three common inorganic anions (Cl^-, NO_3^- and HCO_3^-) on the CLQ degradation was evaluated by using the molar ratio of 15:1 ([Fe(VI)]:[CLQ])

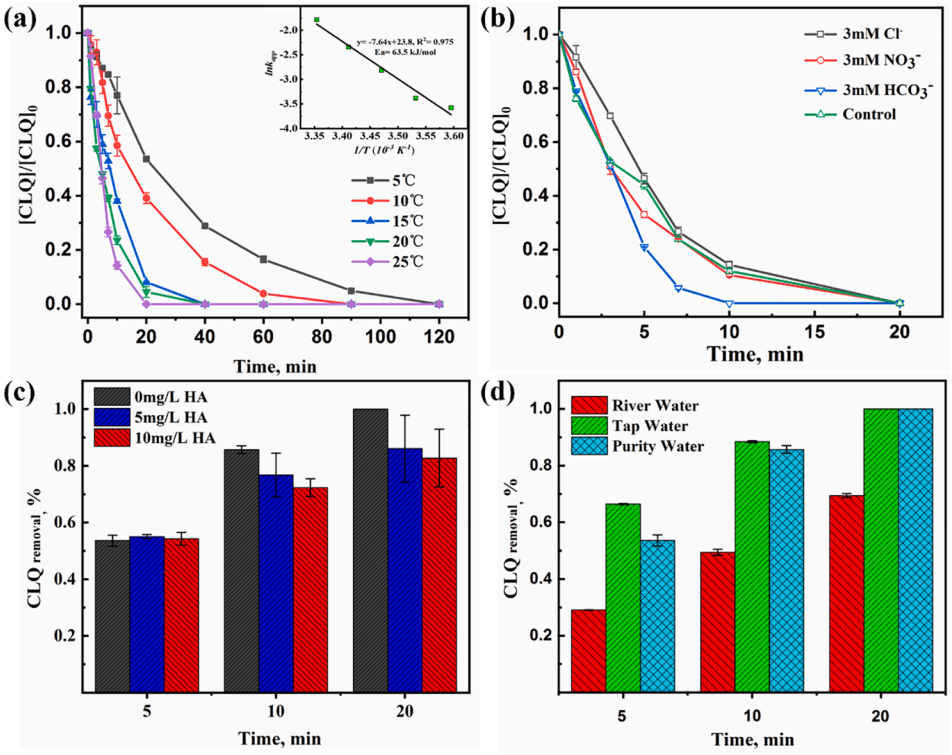

Fig. 3. The effect of temperature (a), inorganic anions (b) and HA (c) on the degradation efficiency of CLQ. (d) The degradation of CLQ in natural waters (The ratio of [Fe(VI)]/[CLQ] = 15:1, initial CLQ concentration = 10 μM, pH = 9.0).

at pH 9.0. The results were depicted in Fig. 3b.

Compared with the control experiment, the effect of Cl^- at the tested concentration (3 mM) had negative impact on CLQ removal at initial 5 min. This result indicated the fact that Cl^- concentrations might affect the dehalogenation during the oxidation of CLQ by Fe(VI), which could not facilitate the degradation of CLQ. Wu et al. also obtained the same conclusion when using Fe(VI) to degrade phenol in chloride ion water [44]. Another explanation might be that the pH value of the reaction solution was decreased with the presence of Cl^- which consumed more amount of Fe(VI) [45]. Besides, the effects of NO_3^- at the tested concentration (3 mM) slightly promoted the CLQ removal at initial 7 min. NO_3^- would act like to retard the decomposition of Fe(VI), and hence slightly favor Fe(VI) oxidation, which agreed well with the result of Schreyer et al. [9]. However, the effects of NO_3^- and Cl^- on the final degradation of CLQ by Fe(VI) were not noticeable. The removal of CLQ could reach 100% within 20 min. This was because of the low reactivity of Fe(VI) with NO_3^- and Cl^-.Feng et al. [33] and Liu et al [46] found that the presence of NO_3^- and Cl^- could not affect the oxidation rate of flumequine and parathion, which was consistent with this result. Moreover, the addition of HCO_3^- significantly accelerated the oxidation of CLQ and Fe(VI). After reaction of 10 min, the removal rate of CLQ reached 100%. HCO_3^- raised the alkalinity and the ionic strength of the reaction system, enhancing the stability of Fe(VI) and improving the utilization efficiency of Fe(VI) [47].

Humic acid (HA) as an essential component of dissolved organic matters (DOM), is unavoidable in nature water. The effect of HA on removal of CLQ by Fe(VI) was shown in Fig. 3c. Compared with the control solution, the removal efficiency of CLQ by Fe(VI) was decreased with the addition of HA. When the solution contained 5 and 10 mg/L HA, the removal efficiencies were decreased to 73% and 63% within 7 min, respectively. HA decreased the oxidation of CLQ with Fe(VI), and the inhibitory effect increased with increasing HA concentrations. HA competed with CLQ to react with Fe(VI), which would consume Fe(VI) and inhibit the removal of CLQ by Fe(VI) in HA-containing water. This result was consistent with previous researches that HA interfered with removing organic chemicals (e.g., flumequine, benzophenone-3) and pharmaceuticals by Fe(VI) [39,45].

In above section, HCO_3^- and HA would affect the degradation of CLQ by Fe(VI). In addition to HCO_3^- and HA, more background ions and dissolved organics existed in natural waters. It is critical to evaluate the feasibility of Fe(VI) oxidation technology for CLQ elimination in real natural waters. Fig. 3d shows the degradation of CLQ with Fe(VI) in tap water and river water. The degradation rate of CLQ decreased as follows: tap water > control water > river water. CLQ was completely removed from tap water and control water within 20 min. In the initial stage, the removal rate of CLQ was faster in tap water might due to the influence of the residual chlorine (Table S1) and coexisting anions (e.g., HCO_3^-). In comparison, the removal efficiency of CLQ only surpassed 73% in river water, which might be attributed to the combined effects of coexisting anions and DOM (Table S1). The slight inhibition of the removal of CLQ in river water required adding more Fe(VI). Overall, Fe(VI) could be used as an efficient technique to degrade co-existing CLQ in natural waters.

3.5. Intermediate products and proposed degradation pathway

The complex transformation products formed during the reaction of CLQ and Fe(VI) were identified by using LC/ESI-QTOF-MS. The total ion current (TIC) chromatograms of the CLQ oxidation by Fe(VI) before and after 120 min are shown in Fig. 4a. Meanwhile, frontier electron density theory and density functional theory (DFT) calculation were combined to determine the intermediate products (e.g., structure) and propose the degradation pathway. Fig. 4b shows the highest occupied molecular orbital (HOMO) of CLQ, and Table S2 shows the $2FED^2_{HOMO}$ values of each atom of CLQ. The frontier orbital theory certified that electrophilic reactions were prone to occur at the atoms with higher $2FED^2_{HOMO}$ values [48]. Therefore, according to the mass spectrums and the NIST MS software analysis, six intermediates were identified in Fig. 4c–h and Table S3.

CLQ has a molecular ion peak of m/z = 320 ($[M + H]^+$). Six

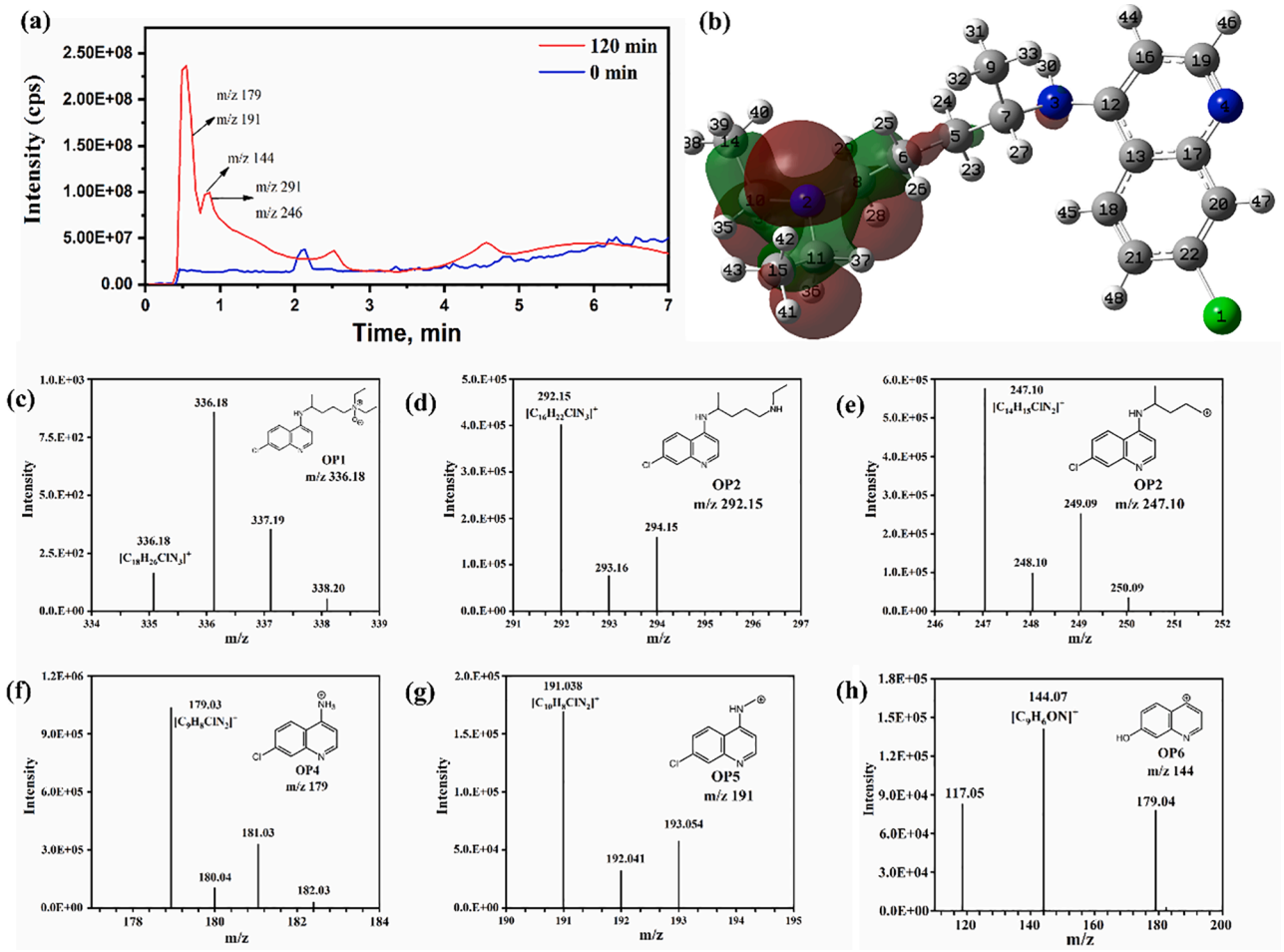

Fig. 4. HPLC/ESI-QTOF-MS chromatograms of the CLQ samples at different reaction time (a), the highest occupied molecular orbital of CLQ (b) and the extracted molecular ion mass/mass spectra of relevant oxidation products (c-h). (The ratio of [Fe(VI)]/[CLQ] = 15:1, initial CLQ concentration = 10 μM, pH = 9.0, T = 25 °C).

intermediates were generated at m/z = 144, 179, 191, 247, 292 and 336. OP1 was identified with the m/z of 336 $(M + H)^+$ in positive mode, which was 16 DA higher than CLQ (320 DA). The addition of 16 DA was corresponded to oxygen and was confirmed as (addition of one oxygen atom) mono N-oxide formation in CLQ, which was consistent with the research of Doddaga et al. [49] OP2 was identified with the m/z of 292 at 0.858 min, attributed to the loss of oxygen atom (–O, 16 DA) and loss of neutral ethylene ($–C_2H_4$) molecule from OP1. In addition, the peak at m/z 247 of OP3 was obtained the β-elimination of the aliphatic chain of the parent ion. The loss of neutral N,N-diethylamine hydroxide resulted in a terminal non-radicalic vinyl group, which protonated at the amine nitrogen. This result was also verified via quantum chemical calculations, where the orbital of HOMO isosurface was mostly distributed above the N,N-diethylamine (Fig. 4b). Besides OP1, OP2 and OP3, three products with m/z values of 191 Da (OP4), 179 Da (OP5) and 144 Da (OP6) were identified in Fig. 4f–h. The highest peak at 0.487 min was identified in the TIC chromatograms as an intermediate product (OP5, m/z = 179). Previous study has reported that OP5 could also be obtained by the reaction between CLQ and hydrogen peroxide [11]. The aromatic ring is prone to dealkylation, which leads to the breaking of the carbon–nitrogen bond [50]. The peak at 0.487 min was identified as OP4 (Fig. 4e), which had a mass of 12 Da higher than that of OP5. OP5 could be considered to be further oxidated by Fe(VI) to break carbon–nitrogen bond of the OP4. The m/z value of the compound arousing the peak at 0.779 min was OP6 (144 Da) (Fig. 4c), 35 Da lower than that of OP5. Based on the product OP6, the chlorine atom could be replaced by a hydroxyl group during the Fe(VI) oxidation of CLQ. The substitution of chlorine atoms was produced by the oxidation reactant of hydroxyl radicals generated by the self-decomposition of Fe (VI) in the buffer solution [37].

According to the above-identified intermediates and the theoretical calculations, a possible pathway of CLQ oxidation by Fe(VI) was proposed in Fig. 5. The degradation of CLQ by Fe(VI) was mainly composed of aromatic ring dealkylation and chloride ion substitution. When Fe(VI) oxidizes organic matter, Fe(V), Fe(IV) and Fe(III) are gradually formed through single electron transfer. Fe(VI) initially attacked the N-diethylamine (electron rich moiety) of CLQ, in which N atom acted an electron pair donor to the high valent Fe(VI) via direct interaction with the ferrate oxygen atoms. The charge carried by N-diethylamine on CLQ was gradually transferred by Fe(VI) in the single electron to form mono N-oxide (OP1) and Fe(III). The reaction process was similar to the previous studies on sulfadiazine by Fe(VI) [51]. Besides, based on the higher $2FED^2_{HOMO}$ value of N(2), electrophilic reactions were prone to occur at the atoms with higher $2FED^2_{HOMO}$ values [48]. Subsequently, these compounds would transform into OP2 through loss of oxygen atom and ethylene ($–C_2H_4$) molecule. Due to protonation at the amine nitrogen of OP2, OP2 was further oxidized by Fe(VI) to form OP3. Then, the aromatic ring of OP3 was dealkylated to form OP4 and OP5. Finally, the

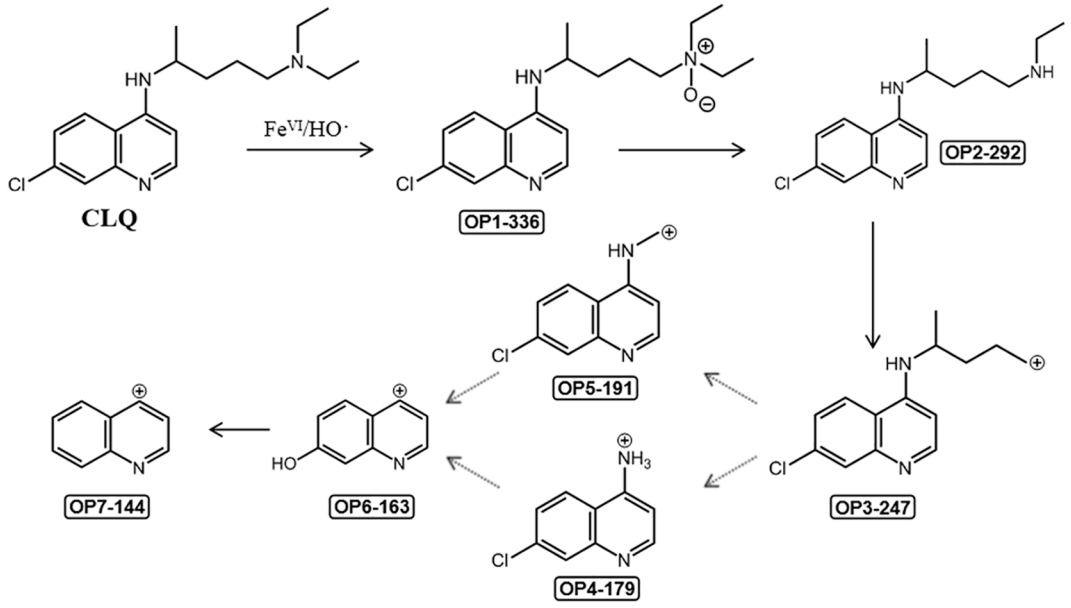

Fig. 5. Proposed degradation pathway of CLQ with Fe(VI). (The ratio of [Fe(VI)]/[CLQ] = 15:1, initial CLQ concentration = 10 μM, pH = 9.0, T = 25 °C).

chlorine atoms of CLQ could be replaced by a hydroxyl group by the oxidation of hydroxyl radicals produced by Fe(VI) self-decomposition to form OP6. Meanwhile, OP6 dealkylated the hydroxyl group to form OP7. Consistent with this work, CLQ was also observed dealkylation with the oxidation of hydrogen peroxide [49].

3.6. Antibacterial activity

Although CLQ could be effectively degraded by Fe(VI), its new intermediate products generated during the degradation process, such as OP6 and OP7, may possess potential biotoxicity. Hence, the CLQ degradation samples by Fe(VI) treatment were inoculated with *E. coli* to examine the antibacterial activity of the CLQ degradation products. Fig. 6 compares the effect of Fe(VI), CLQ and their oxidation products on the growth of *E. coli*. With the inoculation of *E. coli* for 24 h, the value of OD_{600} were 1.355, 1.371 and 1.393 in the control group, Fe(VI) group and CLQ group, respectively. Compared with the control group, the growth of *E. coli* in CLQ group and Fe(VI) group were not obviously affected, indicating that the antimicrobial effect of CLQ (10 μM) on *E. coli* could be ignored. This might due to the fact that CLQ had no significant effect on DNA synthesis in *E. coli*. Meanwhile, Fe(VI) has no antibacterial effect on *E .coli*, which was consistent with the result of Yang et al [52]. However, after treatment by Fe(VI), the peak value of OD_{600} in the CLQ degradation products was lower (1.249) than that of the control group (1.355), suggesting that the biotoxicity of CLQ degradation products towards *E. coli* appeared to be increased. Because the oxidation of CLQ by Fe(VI) further formed the lower molecular weight products containing benzene and pyridine, which exhibited higher toxicity than the CLQ group. EI-Sayed et al. reported that a series of pyridines as antimicrobial agents demonstrated varying antibacterial effects [53]. Therefore, this data further suggested that the CLQ degradation by ferrate would slightly increase the antimicrobial effect towards *E. coli*. In order to comprehensively evaluate the potential aquatic ecological risks of CLQ oxidation, the acute and chronic toxicity of CLQ and its intermediates was calculated by ECOSAR software (Fig. S8). According to the Globally Harmonized System of Classification and Labeling of Chemicals, CLQ and its intermediates have been classified into four categories (not harmful, harmful, toxic, and very toxic). In the acute toxicity, except OP-2, most of the intermediate products were less toxic to fish, daphnid and green algae than CLQ itself. Compared with the acute toxicity, the chronic toxicity of CLQ and intermediate products were increased. But the chronic toxicity of intermediate products was still less than CLQ itself. Thus, the potential toxicity risk of intermediates (e.g., acute toxicity and chronic toxicity) were weakened after the Fe(VI) oxidation.

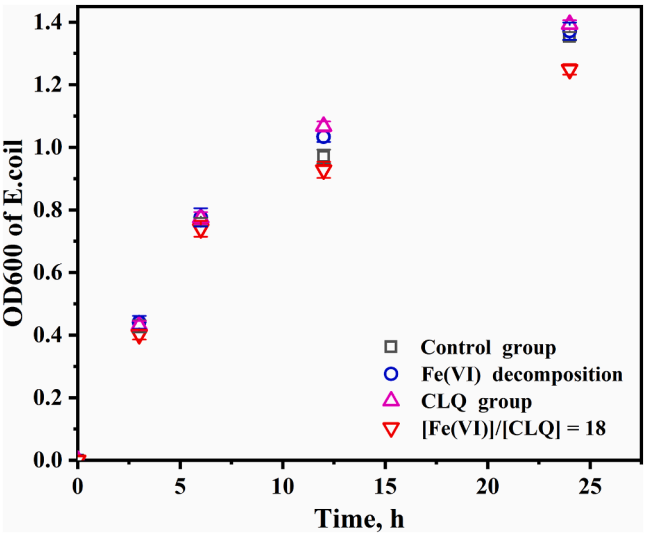

Fig. 6. Growth curve of *E. coli* in control group (diluted LB medium), CLQ group (10 μM), ferrate group (180 μM of ferrate dissolved in pure water, decomposed for 12 h) and ferrate treated CLQ group (10 μM of CLQ oxidized by 180 μM of ferrate for 12 h).

4. Conclusions

This study demonstrated that CLQ could be effectively oxidized by Fe(VI) within minutes in acidic to basic pH range. CLQ was degraded faster with the increasing of the Fe(VI) concentration, which was completely degraded by Fe(VI) with a stoichiometric ratio of 15:1 (Fe(VI):CLQ). The reaction was pH dependent and followed second-order kinetics. The species-specific rate constants determined for the reaction of $HFeO_4^-$ with neutral CLQ and with anionic CLQ were 7.7×10^2 M^{-1} s^{-1} and 0.82×10^2 M^{-1} s^{-1}, respectively. Besides, increasing the reaction temperature would increase the degradation rate of CLQ. Coexisting partial

inorganic anions (e.g., HCO_3^-) and HA could negatively influence the removal of CLQ by Fe(VI). Moreover, based on six oxidation products identified by LC-TOF-MS, a possible mechanism for the oxidation of CLQ by Fe(VI) was proposed, involving aromatic ring dealkylation and chloride ion substitution. Of note, toxicity evolution by luminescence tests and the antimicrobial effects toward *E. coli* showed that the oxidation of CLQ by Fe(VI) could slightly increase potential antibacterial activity.

Declaration of Competing Interest

The authors declare that they have no known competing financial interests or personal relationships that could have appeared to influence the work reported in this paper.

Acknowledgments

This work was financially supported by the Zhejiang Provincial Natural Science Foundation of China (Grants LR21E080001 and LQ21E080011), the National Natural Science Foundation of China (Grants 22076168, 52000158, 22006131 and 21876156) and the Zhejiang Provincial Ten Thousand Talent Program (Grant 2018R52013). Central Government Guided Local Science and Technology Development Fund (2021ZY1022).

Appendix A. Supplementary data

Supplementary data to this article can be found online at https://doi.org/10.1016/j.cej.2021.131408.

References

[1] H. Barabadi, Z. Alizadeh, M.T. Rahimi, A. Barac, A.E. Maraolo, L.J. Robertson, A. Masjedi, F. Shahrivar, E. Ahmadpour, Nanobiotechnology as an emerging approach to combat malaria: a systematic review, Nanomedicine Nanotechnology, Biol. Med. 18 (2019) 221–233.
[2] A.F. Cowman, J. Healer, D. Marapana, K. Marsh, Malaria: biology and disease, Cell 167 (2016) 610–624.
[3] N. Tangpukdee, C. Duangdee, P. Wilairatana, S. Krudsood, Malaria diagnosis: a brief review, Korean J. Parasitol. 47 (2) (2009) 93, https://doi.org/10.3347/kjp.2009.47.2.93.
[4] R.R. Das, N. Jaiswal, N. Dev, N. Jaiswal, S.S. Naik, J. Sankar, Efficacy and safety of anti-malarial Drugs (Chloroquine and Hydroxy-Chloroquine) in treatment of COVID-19 infection: a systematic review and meta-analysis, Front. Med. 7 (2020) 482.
[5] K. Yuki, M. Fujiogi, S. Koutsogiannaki, COVID-19 pathophysiology: a review, Clin. Immunol. 215 (2020) 108427, https://doi.org/10.1016/j.clim.2020.108427.
[6] M. Park, A.R. Cook, J.T. Lim, Y. Sun, B.L. Dickens, A systematic review of COVID-19 Epidemiology based on current evidence, J. Clin. Med. 9 (4) (2020) 967, https://doi.org/10.3390/jcm9040967.
[7] C. Coban, The host targeting effect of chloroquine in malaria, Curr. Opin. Immunol. 66 (2020) 98–107.
[8] J.O. Olatunde, A. Chimezie, B. Tolulope, T.T. Aminat, Determination of pharmaceutical compounds in surface and underground water by solid phase extraction-liquid chromatography, J. Environ. Chem. Ecotoxicol. 6 (3) (2014) 20–26.
[9] S. Jm, O. Lt, Stability of the ferrate(VI) ion in aqueous solution, Anal. Chem. 23 (1951) 1312–1314.
[10] X.-H. Yi, H. Ji, C.-C. Wang, Y. Li, Y.-H. Li, C. Zhao, A.o. Wang, H. Fu, P. Wang, X. u. Zhao, W. Liu, Photocatalysis-activated SR-AOP over PDINH/MIL-88A(Fe) composites for boosted chloroquine phosphate degradation: Performance, mechanism, pathway and DFT calculations, Appl. Catal. B Environ. 293 (2021) 120229, https://doi.org/10.1016/j.apcatb.2021.120229.
[11] S. Midassi, A. Bedoui, N. Bensalah, Efficient degradation of chloroquine drug by electro-Fenton oxidation: Effects of operating conditions and degradation mechanism, Chemosphere 260 (2020), 127558.
[12] M.P. Chipperfield, R. Hossaini, S.A. Montzka, S. Reimann, D. Sherry, S. Tegtmeier, Renewed and emerging concerns over the production and emission of ozone-depleting substances, Nat. Rev. Earth Environ. 1 (5) (2020) 251–263.
[13] L.M. Polvani, M. Previdi, M.R. England, G. Chiodo, K.L. Smith, Substantial twentieth-century Arctic warming caused by ozone-depleting substances, Nat. Clim. Change 10 (2) (2020) 130–133.
[14] A. Sharma, D. Kapoor, J. Wang, B. Shahzad, V. Kumar, A.S. Bali, S. Jasrotia, B. Zheng, H. Yuan, D. Yan, Chromium bioaccumulation and its impacts on plants: an overview, Plants 9 (1) (2020) 100, https://doi.org/10.3390/plants9010100.
[15] N. Rubalingeswari, D. Thulasimala, L. Giridharan, V. Gopal, N.S. Magesh, M. Jayaprakash, Bioaccumulation of heavy metals in water, sediment, and tissues of major fisheries from Adyar estuary, southeast coast of India: an ecotoxicological impact of a metropolitan city, Mar. Pollut. Bull. 163 (2021), 111964.
[16] S. Bodur, S. Erarpat, Ö.T. Günkara, S. Bakırdere, Development of an easy and rapid analytical method for the extraction and preconcentration of chloroquine phosphate from human biofluids prior to GC–MS analysis, J. Pharmacol. Toxicol. Methods 108 (2021), 106949.
[17] A. Cheomung, K. Na-Bangchang, HPLC with ultraviolet detection for the determination of chloroquine and desethylchloroquine in whole blood and finger-prick capillary blood dried on filter paper, J. Pharm. Biomed. Anal. 55 (5) (2011) 1031–1040.
[18] Z. Guoquan, W. Tinggong, S. Danfeng, S. Jian, Y. Zehui, The solubility and dissolution thermodynamic properties of chloroquine diphosphate in different organic solvents, J. Chem. Thermodyn. 156 (2021), 106368.
[19] K. Nord, J. Karlsen, H.H. Tønnesen, Photochemical stability of biologically active compounds. IV. Photochemical degradation of chloroquine, Int. J. Pharm. 72 (1) (1991) 11–18.
[20] Y. Lee, U. von Gunten, Oxidative transformation of micropollutants during municipal wastewater treatment: Comparison of kinetic aspects of selective (chlorine, chlorine dioxide, ferrateVI, and ozone) and non-selective oxidants (hydroxyl radical), Water Res. 44 (2010) 555–566.
[21] V.K. Sharma, Oxidation of inorganic contaminants by ferrates (VI, V, and IV)–kinetics and mechanisms: a review, J. Environ. Manage. 92 (2011) 1051–1073.
[22] J. Ma, W. Liu, Effectiveness and mechanism of potassium ferrate(VI) preoxidation for algae removal by coagulation, Water Res. 36 (4) (2002) 871–878.
[23] Q. Zheng, N. Wu, R. Qu, G. Albasher, W. Cao, B. Li, N. Alsultan, Z. Wang, Kinetics and reaction pathways for the transformation of 4-tert-butylphenol by ferrate(VI), J. Hazard. Mater. 401 (2021), 123405.
[24] Y. Li, L. Jiang, R. Wang, P. Wu, J. Liu, S. Yang, J. Liang, G. Lu, N. Zhu, Kinetics and mechanisms of phenolic compounds by Ferrate(VI) assisted with density functional theory, J. Hazard. Mater. 415 (2021), 125563.
[25] Y. Lee, S.G. Zimmermann, A.T. Kieu, U. von Gunten, Ferrate (Fe(VI)) application for municipal wastewater treatment: a novel process for simultaneous micropollutant oxidation and phosphate removal, Environ. Sci. Technol. 43 (2009) 3831–3838.
[26] V.K. Sharma, Potassium ferrate(VI): an environmentally friendly oxidant, Adv. Environ. Res. 6 (2002) 143–156.
[27] V.K. Sharma, L. Chen, R. Zboril, Review on high valent FeVI (Ferrate): a sustainable green oxidant in organic chemistry and transformation of pharmaceuticals, ACS Sustain. Chem. Eng. 4 (2016) 18–34.
[28] A.H. Alshahri, L. Fortunato, N. Ghaffour, T. Leiknes, Controlling harmful algal blooms (HABs) by coagulation-flocculation-sedimentation using liquid ferrate and clay, Chemosphere 274 (2021), 129676.
[29] A. Talaiekhozani, M.R. Talaei, S. Rezania, An overview on production and application of ferrate (VI) for chemical oxidation, coagulation and disinfection of water and wastewater, J. Environ. Chem. Eng. 5 (2) (2017) 1828–1842.
[30] A.H. Alshahri, L. Fortunato, NorEddine Ghaffour, TorOve Leiknes, Advanced coagulation using in-situ generated liquid ferrate, Fe (VI), for enhanced pretreatment in seawater RO desalination during algal blooms, Sci. Total Environ. 685 (2019) 1193–1200.
[31] O. Monfort, M. Usman, K. Hanna, Ferrate(VI) oxidation of pentachlorophenol in water and soil, Chemosphere. 253 (2020), 126550.
[32] B. Ni, X. Yan, X. Dai, Z. Liu, W. Wei, S. Wu, Q. Xu, J. Sun, Ferrate effectively removes antibiotic resistance genes from wastewater through combined effect of microbial DNA damage and coagulation, Water Res. 185 (2020), 116273.
[33] M. Feng, X. Wang, J. Chen, R. Qu, Y. Sui, L. Cizmas, Z. Wang, V.K. Sharma, Degradation of fluoroquinolone antibiotics by ferrate(VI): effects of water constituents and oxidized products, Water Res. 103 (2016) 48–57.
[34] Q. Han, W. Dong, H. Wang, T. Liu, Y. Tian, X. Song, Degradation of tetrabromobisphenol A by ferrate(VI) oxidation: Performance, inorganic and organic products, pathway and toxicity control, Chemosphere 198 (2018) 92–102.
[35] T. Yang, L. Wang, Y. Liu, W. Zhang, H. Cheng, M. Liu, J. Ma, Ferrate oxidation of bisphenol F and removal of oxidation products with ferrate resulted particles, Chem. Eng. J. 383 (2020), 123167.
[36] C. Li, X.Z. Li, N. Graham, A study of the preparation and reactivity of potassium ferrate, Chemosphere 61 (4) (2005) 537–543.
[37] Y. Lee, R. Kissner, U. von Gunten, Reaction of ferrate(VI) with ABTS and self-decay of ferrate(VI): kinetics and mechanisms, Environ. Sci. Technol. 48 (9) (2014) 5154–5162.
[38] L.u. Wang, Y. Liu, J. Ma, F. Zhao, Rapid degradation of sulphamethoxazole and the further transformation of 3-amino-5-methylisoxazole in a microbial fuel cell, Water Res. 88 (2016) 322–328.
[39] G.A.K. Anquandah, V.K. Sharma, D.A. Knight, S.R. Batchu, P.R. Gardinali, Oxidation of trimethoprim by ferrate(VI): kinetics, products, and antibacterial activity, Environ. Sci. Technol. 45 (2011) 10575–10581.
[40] H. Dong, Z. Qiang, S. Liu, J. Li, J. Yu, J. Qu, Oxidation of iopamidol with ferrate (Fe (VI)): kinetics and formation of toxic iodinated disinfection by-products, Water Res. 130 (2018) 200–207.
[41] C. Luo, M. Feng, V.K. Sharma, C. Huang, Revelation of ferrate(VI) unimolecular decay under alkaline conditions: Investigation of involvement of Fe(IV) and Fe(V) species, Chem. Eng. J. 388 (2020), 124134.
[42] W. Wanger, J. Gump, E. Hart, Factors affecting the stability of aqueous potassium ferrate(VI) solutions, Anal. Chem. 9 (1952) 1497–1498.

[43] X. Yang, P.-F. Tian, C. Zhang, Y.-Q. Deng, J. Xu, J. Gong, Y.-F. Han, Au/carbon as Fenton-like catalysts for the oxidative degradation of bisphenol A, Appl. Catal. B Environ. 134-135 (2013) 145–152.
[44] D. Wu, Y. Xiong, M. He, S. Yang, J. Cai, Z. Wu, S. Sun, X. Chen, W.D. Wu, Determination of phenol degradation in chloride ion rich water by ferrate using a chromatographic method in combination with on-line mass spectrometry analysis, Anal. Methods 11 (36) (2019) 4651–4658.
[45] B. Yang, G.-G. Ying, Oxidation of benzophenone-3 during water treatment with ferrate(VI), Water Res. 47 (7) (2013) 2458–2466.
[46] H. Liu, X. Pan, J. Chen, Y. Qi, R. Qu, Z. Wang, Kinetics and mechanism of the oxidative degradation of parathion by Ferrate(VI), Chem. Eng. J. 365 (2019) 142–152.
[47] N. Graham, C.-C. Jiang, X.-Z. Li, J.-Q. Jiang, J. Ma, The influence of pH on the degradation of phenol and chlorophenols by potassium ferrate, Chemosphere 56 (10) (2004) 949–956.
[48] T. Zhang, G. He, F. Dong, Q. Zhang, Y. Huang, Chlorination of enoxacin (ENO) in the drinking water distribution system: Degradation, byproducts, and toxicity, Sci. Total Environ. 676 (2019) 31–39.
[49] S. Doddaga, R. Peddakonda, Chloroquine-N-oxide, a major oxidative degradation product of chloroquine: Identification, synthesis and characterization, J. Pharm. Biomed. Anal. 81-82 (2013) 118–125.
[50] Y. Xu, J. Radjenovic, Z. Yuan, B. Ni, Biodegradation of atenolol by an enriched nitrifying sludge: products and pathways, Chem. Eng. J. 312 (2017) 351–359.
[51] H. Wang, S. Wang, J. Jiang, J. Shu, Removal of sulfadiazine by ferrate(VI) oxidation and montmorillonite adsorption—Synergistic effect and degradation pathways, J. Environ. Chem. Eng. 7 (2019), 103225.
[52] T. Yang, L. Wang, Y. Liu, Z. Huang, H. He, X. Wang, J. Jiang, D. Gao, J. Ma, Comparative study on ferrate oxidation of BPS and BPAF: Kinetics, reaction mechanism, and the improvement on their biodegradability, Water Res. 148 (2019) 115–125.
[53] H.A. El-Sayed, A.H. Moustafa, A.E. El-Torky, E.A. Abd El-Salam, A series of pyridines and pyridine based sulfa-drugs as antimicrobial agents: Design, synthesis and antimicrobial activity, Russ. J. Gen. Chem. 87 (2017) 2401–2408.